

Dear Editor:

Thank you for pointing out the mistakes in the draft. We have made revision accordingly to address the comments below. We also made thorough proof reading to avoid grammar mistakes and make the paper flow better.

abstract: "... a Rossby wave train originates from western Pacific and propagates into midlatitude over North America ...". Need "the" before "western" and "midlatitude" should be "midlatitudes".

We have made these changes.

Figure 7: put plots on top of each other to make them larger - all axes/title text are too small.
We have repositioned the figures accordingly.

Format references so there are clear breaks between each article.

The references are separated by a line break between them now.

line 281 discussion: "the precipitation in the Western Canadian Prairie ...". "Prairie" should be "Prairies".

We have corrected the spelling here and many other similar errors.

line 282 discussion: "... more extended dry spells tend to occur in Canadian Prairies during ...". Need "the" before Canadian.

We have added "the" before Canada and similar places in the paper.

line 311 discussion: "... MJO-4 index cannot determine the sign of precipitation anomaly in the Prairies alone." Need "the" before "precipitation".

We have added "the" before "precipitation".

lines 330-332, Conclusion: This entire first sentence has poor grammar.

We have rephrased the sentence.

line 333 conclusions: "... through the propagation of stationary Rossby wave from the western Pacific ...". Wave should be "waves".

We have changed the word to the plural form.

line 342 conclusions: "... can propagate into western Canada if they oriented relatively zonally." Need "are" before "oriented".

We have added "are" before "oriented".

Combined Impacts of ENSO and MJO on the 2015 Growing Season Drought on the Canadian Prairies

Zhenhua Li^{1,2}, Yanping Li¹, Barrie Bonsal³, Alan H. Manson², Lucia Scaff¹

¹Global Institute for Water Security, University of Saskatchewan, Saskatoon, Saskatchewan, Canada S7N 3H5

²Institute of Space and Atmospheric Studies, University of Saskatchewan, Saskatoon, Saskatchewan, Canada.

³National Hydrology Research Center, Environment and Climate Change Canada, Saskatoon, SK, Canada

Correspondence to: Dr. Yanping Li (yanping.li@usask.ca); Dr. Zhenhua Li (zhenhua.li@usask.ca)

Abstract

Warm-season precipitation on the Canadian Prairies plays a crucial role in agricultural production. This research investigates how the early summer 2015 drought across the Canadian Prairies is related to the tropical Pacific forcing. The ant deficit of precipitation in May and June 2015 coincided with a warm phase of El Niño-Southern Oscillation (ENSO) and a negative phase of Madden-Julian Oscillation (MJO)-4 index, which favour a positive geopotential height anomaly in western Canada. Our further investigation during the instrumental record (1979-2016) shows that warm-season precipitation in the Canadian Prairies and the corresponding atmospheric circulation anomalies over western Canada are connected with the lower boundary conditions in the tropical western Pacific. Our results indicate that MJO can play a role in determining the summer precipitation anomaly in the western Canadian Prairies when the equatorial central Pacific is warmer than normal ($\text{NINO4} > 0$) and MJO is more active. This teleconnection is due to the propagation of a stationary Rossby wave that is generated in the MJO-4 index region. When the tropical convection around MJO-4 index

region (western tropical Pacific, centred over 140°E) is more active than normal (NINO4 > 0), Rossby wave trains originate from the western Pacific with wavenumbers determined by the background mean wind and meridional absolute vorticity gradient. Under warm NINO4 conditions waves are generated with smaller wavenumbers compared to cold NINO4 conditions. These waves under warm NINO4 can propagate into the midlatitudes over North America causing a persistent anomalous ridge in the upper level over western Canada, which favours dry conditions over the region.

Deleted:

Deleted: of

Deleted: centered

Deleted: ◊

Deleted: a

Deleted: train originates

Deleted: propagates

Deleted: midlatitud

Deleted:

33 1 Introduction

34 The Canadian Prairies depend on summer precipitation especially during the early to mid-
35 growing season (May through August) when the majority of annual precipitation normally occurs (e.g.,
36 Bonsal *et al.* 1993). High natural variability in growing season precipitation causes periodic occurrences
37 of extreme precipitation (Li *et al.* 2017; Liu *et al.* 2016) and droughts that are often associated with
38 reduced agriculture yields, low streamflow, and increased occurrence of forest fires (Wheaton *et al.*
39 2005, Bonsal and Regier 2007). Drought events with great environmental and economic impacts on the
40 Canadian Prairies have occurred in 1961, 1988, 2001-2002, and as recent as 2015 (Dey 1982, Liu *et al.*
41 2004, Bonsal *et al.* 1999, Wheaton *et al.* 2005, Shabbar *et al.* 2011, Bonsal *et al.* 2013, Szeto *et al.*
42 2016). The sub-seasonal forecast of precipitation for the growing season is crucial for the agriculture,
43 water resource management, and the economy of the region. Therefore, an investigation into the causes
44 of inter-annual variability in the growing season precipitation of the Canadian Prairie is needed.

45 Low precipitation and extended dry periods on the Canadian Prairies are often associated with an
46 upper-level ridge and a persistent high pressure centred over the region (Dey 1982, Liu *et al.* 2004).
47 These prolonged atmospheric anomalies often concurred with abnormal boundary layer conditions such
48 as a large-scale sea surface temperature (SST) anomalies in the Pacific Ocean (Shabbar and Skinner
49 2004). Large-scale oscillation in the SST anomalies in the Pacific Ocean, namely El Nino, and the
50 Pacific Decadal Oscillation (PDO), can affect the hydroclimatic pattern in summer over North America,
51 although the strongest impacts of these boundary conditions occur during the boreal winter. Inter-annual
52 variability such as El Nino-Southern Oscillation (ENSO) is linked with extended droughts in the Prairies
53 (Bonsal *et al.* 1999, Shabbar and Skinner 2004). Interdecadal oscillations such as the PDO, and the
54 Atlantic Multi-decadal Oscillation (AMO) also affect the seasonal temperature and precipitation in the
55 Canadian Prairies (Shabbar *et al.* 2011).

Deleted: depends

Deleted: centered

Deleted:

Deleted:

60 ENSO's relationship with the Canadian Prairies' precipitation has been studied extensively.
61 Previous investigations (e.g., Shabbar *et al.* (2011)) have found that El Nino events are associated with a
62 summer moisture deficit in western Canada while La Nina events cause an abundance of moisture in far
63 western Canada (British Columbia and Yukon). However, they also noted that although tropical SST
64 variability accounted for some aspects of the large-scale circulation anomalies that influence the
65 Canadian Prairies meteorological drought, a consistent and clear-cut relationship was not found. The
66 warm phase of ENSO often favours drought in this region, especially during the growing season after
67 the mature phase of El Nino (Bonsal and Lawford 1999, Shabbar and Skinner 2004). The positive
68 North Pacific Mode (NPM, Hartmann *et al.* 2015) like North Pacific SST anomaly pattern often follows
69 a matured El Nino, and the accompanying atmospheric ridging leads to extended dry spells over the
70 Prairies during the growing season (Bonsal and Lawford 1999). Furthermore, in association with the
71 recent North Pacific SST anomaly from 2013 to 2014, researchers have attributed the precipitation
72 deficit in California during 2013 to the anomalous upper-level ridge over western North America (Wang
73 *et al.* 2014, Szeto *et al.* 2016).

Deleted: Prairie

Deleted: The warm phase of ENSO often favours drought in this region, especially during the growing season after the mature phase of El Nino with the North Pacific Mode (NPM, Hartmann *et al.* 2015) positive like North Pacific SST anomaly pattern (Bonsal and Lawford 1999, Shabbar and Skinner 2004).

Deleted: warm anomalies, which

Deleted: follow

Deleted: the

Deleted:

Deleted:

74 The aforementioned SST variations mostly vary on inter-annual and decadal scales. Another
75 important factor that affects the weather patterns in North America is the Madden-Julian Oscillation
76 (MJO), an intra-seasonal (40-90 days) oscillation in convection and precipitation pattern over the
77 Tropics (Madden and Julian 1971, Zhang 2005, Riddle *et al.* 2013, Carbone and Li 2015). MJO is a
78 coupled atmosphere-ocean oscillation involving convection and large-scale equatorial waves, which
79 produces an eastward propagation of tropical convection anomaly (Madden and Julian 1971). The MJO
80 affects the winter temperature and precipitation in North America and Europe through its impact on
81 moisture transport associated with the “Pineapple Express” and its effects on the North Atlantic
82 Oscillation and stratospheric polar vortex (Cassou 2008, Garfinkel *et al.* 2012, Rodney *et al.* 2013).
83 MJO is also connected to the summer precipitation anomalies in the Southwest United States (Lorenz

96 and Hartmann 2006). During the warm season, MJO's impact on the Canadian Prairies' precipitation has
97 not been thoroughly investigated as MJO's amplitude is weak during spring and early summer. The
98 amplitude of MJO in spring and early summer is related to the inter-annual variation of tropical SST,
99 especially the SST in central Pacific (Hendon *et al.* 2007, Marshall *et al.* 2016). MJO in terms of the
100 Real-time Multivariate MJO index (RMM, Wheeler and Hendon 2004), was extremely strong in the
101 early spring of 2015 with a positive PDO-like SST anomaly in the central Pacific and at the same time,
102 El Nino started to strengthen.

Deleted: Prairie

Deleted: MJO's

Deleted:

103 MJO activities in the western Pacific under the modulation of inter-annual SST variability have
104 the potential to act together with ENSO and impact mid-tropospheric circulation over western Canada
105 and thus, warm season precipitation over the Canadian Prairies. The goal of this study is to demonstrate
106 that MJO has contributed to the 2015 growing season drought in the Canadian Prairies through the
107 propagation of stationary Rossby wave. Subsequently, further investigations are carried out to determine
108 if similar relationships exist in association with other summer extreme precipitation events during
109 instrumental record (1979-2016). Section 2 provides the datasets and methodology used in this paper
110 while section 3 presents the analysis of the upper-level circulation anomaly and SST pattern associated
111 with the 2015 drought. This is followed by the examination of the effects of central Pacific SST
112 anomalies and MJO on the summer precipitation in the Canadian Prairies. The mechanism by which
113 MJO affects summer precipitation when equatorial central Pacific SST is warmer than normal is
114 discussed in section 4 followed by the summary and concluding remarks in section 5.

Deleted: have

Deleted: a

115 **2 Data and Methodology**

116 Multiple observation and reanalysis datasets are used to investigate the circulation anomalies
117 associated with the Canadian Prairies' growing season (May-August) precipitation. The observed
118 precipitation is taken from the Climate Prediction Center (CPC) Merged Analysis of Precipitation

Deleted: Prairie

Deleted: Observed

126 (CMAP) dataset (Xie and Arkin 1997). Geopotential height fields from the National Center for

127 Environmental Predictions (NCEP) Reanalysis (Kalnay *et al.* 1996) and the European Center for

128 Medium-Range Weather Forecast (ECMWF)'s ERA-Interim reanalysis (Dee *et al.* 2011) are used to

129 analyze the mid- and upper-level (500 hPa and 200 hPa) atmospheric circulation patterns.

130 To represent the central Pacific SST anomaly, NINO4 SST index (Rayner *et al.* 2003) from CPC

131 of National Oceanic and Atmospheric Administration (NOAA) is used since the NINO4 region is near

132 the central Pacific and spans over the dateline (5°S-5°N, 160°E-150°W). Multivariate ENSO Index

133 (MEI) data are retrieved from NOAA's Climate Data Center (CDC) website and is used to determine the

134 ENSO phase (Wolter 1987, Wolter and Timlin 1993). In particular, El Nino condition is defined when

135 the monthly mean index of MEI is larger than 0.5 (Andrews *et al.* 2004).

136 The Real-time Multivariate MJO series (RMM1 and RMM2) developed by Wheeler and Hendon

137 (2004) are used to identify periods of strong MJO activity as the MJO amplitudes are directly calculated

138 by the square root of RMM1 + RMM2. For MJO intensities over the investigated regions, we used the

139 monthly averaged pentad MJO indices from NOAA CPC's MJO index (Xue *et al.* 2002), which have 10

140 indices representing locations around the globe. The CPC's MJO index is based on Extended Empirical

141 Orthogonal Function (EOF) analysis on pentad velocity potential at 200 hPa. Ten MJO indices on a

142 daily scale are constructed by projecting the daily (0000 UTC) velocity potential anomalies at 200 hPa

143 (CHI200) onto the ten time-lagged patterns of the first EOF of pentad CHI200 anomalies (Xue *et al.*

144 2002). Negative values of ten MJO indices correspond to enhanced convection in the 10 regions centred

145 on 20°E, 70°E, 80°E, 100°E, 120°E, 140°E, 160°E, 120°W, 40°W and 10°W in the tropics. MJO indices

146 usually vary between -2 to 2 with negative values indicating above average convective activities in the

147 corresponding region. Because boreal summer usually corresponds to a period of a weaker amplitude of

148 MJO than the winter, we chose the monthly mean value of -0.3 as the criterion of strong convection

149 which is connected to MJO as the index generally vary between -1 and 1. An MJO-4 index (centred on

Deleted: 's

Deleted:

Deleted: and 500 hPa

Deleted:

Deleted: °

Deleted: °

Deleted: °

Deleted: °

Deleted:

Deleted: centered

Deleted: °

Deleted:

Deleted: °

Deleted: centered

171 140°E) of less than -0.3 was considered a relatively strong convection in the western Pacific, which has
172 been found to be a source region of stationary Rossby waves (Simmons 1980). SST observations include
173 Extended Reconstructed Sea Surface Temperature (ERSST) v4 (Huang *et al.* 2015). Outward Longwave
174 Radiation (OLR) data from NOAA Interpolated Outgoing Longwave Radiation are used to ~~derive~~ the
175 composite of anomalies of OLR for a certain phase of MJO.

Deleted: °

Deleted: derived

Deleted:

176 Our study focuses on ~~the~~ growing season precipitation in the provinces of Alberta and
177 Saskatchewan in the Canadian Prairies, where the largest deficits were observed in 2015. Specifically,
178 the regional mean precipitation over 115°-102.5°W, 50°-57.5°N is used (boxed area in Fig. 1, top panel)
179 to represent the Canadian Prairies east of the Rocky Mountains and south of the boreal forest. The
180 ~~chosen~~ region also covers most of the arable land in the Canadian Prairies. Considering the unique
181 MJO-4 and NINO4 indices for 2015, the relationship between the ~~Prairies'~~ warm season (May-August)
182 precipitation with MJO-4 and ENSO during the instrumental records are investigated using correlation
183 and regression. Though the dry months of the 2015 growing season are May and June when MJO-4 was
184 in negative phase, we want to study the statistical relationship between MJO-4 and the ~~Prairies'~~
185 precipitation in ~~the whole period of~~ growing season (May-August). The possible mechanism behind the
186 correlation between MJO-4 and the ~~Prairies'~~ warm season precipitation ~~under~~ El Nino condition is
187 further investigated by analyzing the upper-level circulation associated with convection in the tropical
188 Pacific and stationary Rossby waves in mid-latitudes.

Deleted: °-

Deleted: °

Deleted: °-

Deleted: °

Deleted: chosen

Deleted: Prairies'

Deleted: Prairies'

Deleted: Prairies'

Deleted: during

189

202 **3 Results**

203 **3.1 The 2015 Summer Drought**

204 Almost all of western Canada including British Columbia, the southern Northwest Territories,
205 Alberta, and Saskatchewan had negative precipitation anomalies during May and June 2015. The top
206 plot in Fig. 1 shows the precipitation anomaly in percentage relative to the climatology (1981-2010
207 long-term mean) in Canada during May and June 2015. The bottom plot in Fig. 1 presents the monthly
208 precipitation anomaly averaged over the region encompassed by the dash lines (top panel in Fig. 1). The
209 average annual cycle of the regional precipitation has a dry period between February and May and June
210 has the largest precipitation in all months. The May and June 2015 precipitation deficit was also
211 accompanied by a relatively dry period from February to April [Fig. 1 and Szeto *et al.* 2016], which
212 added to the drought conditions.

Deleted:

213 The 500 hPa geopotential height (GHP) anomaly averaged in May and June are examined
214 together with SST anomaly and ENSO, MJO-4 indices for 2014 and 2015. The 500 hPa GPH anomaly
215 for May and June 2015 shows strong positive anomalies near Alaska and the British Columbia coast
216 (Fig. 2), which is consistent with the findings for other episodes of growing season droughts (e.g., Dey
217 1982; Bonsal and Wheaton, 2005). Accompanying this anomalous ridge, are above normal SSTs in the
218 northeast Pacific off the coast of North America and the central-eastern Pacific (Fig. 3). Both ENSO and
219 the NPM are in positive phases that correspond to a warmer SST near the Pacific coast of North
220 America, consistent with the positive GPH anomalies in western Canada and Alaska. The ridge in
221 Alaska/Bering Straits and the one near British Columbia coast have been previously associated with El
222 Nino and North Pacific SST anomaly such as NPM (Shabbar *et al.* 2011). The monthly mean anomalous
223 ridge prevents storms from reaching the British Columbia coast and the Canadian Prairies causing
224 extended dry spells. Therefore, the GPH anomaly in early growing season in 2015 is consistent with the

Deleted: mid- and upper-level

Deleted: corresponds

229 precipitation anomaly in these regions. The anomalous upper-level ridge in the Western United States
230 and Canada in 2014 and 2015 have also been associated with the developing El Nino and the other main
231 components of Pacific SST variation such as NPM by several recent studies (Hartmann *et al.* 2015, Lee
232 *et al.* 2015, Li *et al.* 2017).

233 The SST anomaly and the associated oscillations/modes, especially ENSO, show consistent
234 agreement with the observed GPH anomaly pattern. The average SST anomaly during the growing
235 season (May-June, July-August) of 2015 shows a persistent strong positive anomaly in the northeast and
236 eastern equatorial Pacific (Fig. 3), which corresponds to the warm phase of NPM and ENSO. SSTs in
237 the eastern tropical Pacific warmed increasingly since the end of 2014 and qualified as an El Nino in
238 early 2015. The NPM became positive in fall 2013, turned exceptionally strong in 2014 and persisted to
239 2015 (Hartmann 2015). The anomalous ridge is concurrent with strong SST anomalies in the tropical
240 Pacific and extratropical North Pacific. NPM, as the third EOF of Pacific SST (30°S-65°N), has also a
241 strong connection to the anomalous ridge in western North America and trough in the eastern US and
242 Canada in 2013-2014 winter (Hartmann 2015, Lee *et al.* 2015). During the ENSO-neutral condition in
243 2013 and 2014, the precursor of ENSO, the so-called “footprinting” mechanism is considered to cause
244 this anomalous ridge in western North America (Wang *et al.* 2014).

245 The variation of the Canadian Prairies' precipitation and its relationship with NINO4 and MJOs
246 are shown in Fig. 4. The time series of monthly RMM amplitude, NINO4 index, MJO-4 indices and the
247 Canadian Prairies' precipitation anomaly from January 2014 to December 2015 shows the atmospheric-
248 oceanic circulation indices for the drought in 2015. In May and June 2015, the western Pacific witnessed
249 a strong MJO-4 negative index, whereas in July the MJO-4 index became positive. This corresponds
250 well with the precipitation anomaly in Fig. 1. As shown in Fig. 3, El Nino continued to strengthen in
251 July and August 2015; while at the same time the MJO-4 index increased. The increase of the MJO-4
252 index indicated that the active convection associated with MJO moved away from the tropical western

264 Pacific region and propagated eastward into the central Pacific. Coincident with this change in MJO, the
265 precipitation in the Canadian Prairies then returned to slightly above normal in July. Deleted:

266 The good correspondence of MJO-4 and the negative precipitation anomaly suggests a link
267 between MJO and Prairie precipitation during the growing season. Although El Nino and associated
268 Northeast Pacific SST warm anomaly (i.e., NPM) in summer 2015 can be a contributing factor for the
269 persistent upper-level ridge over the west coast of Canada. (Shabbar et al. 2011), it cannot fully explain
270 the drought condition in western Canada, as these SSTs do not guarantee a prolonged dry spell as shown
271 by correlation analysis (Table 1). The negative MJO-4 index concurred with the negative anomaly of the
272 Prairies' growing season precipitation in 2015, which prompts the investigation of their relationship
273 with the instrumental records.

274

275 **3.2 Instrumental record**

276 El Nino and its associated North Pacific SST anomaly may contribute to extended dry spells in
277 Canadian Prairies after the mature phase of El Nino (Bonsal *et al.* 1993) on an inter-annual time scale.
278 ENSO, however, is not a strong intra-seasonal to seasonal predictor of Canadian Prairie summer
279 precipitation. The lack of a strong correlation between the Prairies' precipitation and ENSO index can
280 be caused by the fact that many factors can affect the Prairies' precipitation on a seasonal and sub-
281 seasonal scale. Shabbar and Skinner (2004) showed the connection between the warm phase of ENSO
282 and western Canadian drought through singular value decomposition analysis. However, they also found
283 other modes of SST variation (e.g., the positive phase of PDO) can produce a wet condition in the
284 Prairies. Here we present a new result showing that under warm central Pacific SST conditions
285 (NINO4 > 0), a certain phase of MJO, which connected to the active convection in the tropical western

292 Pacific (Li and Carbone 2012), plays an important role in modulating the growing season precipitation
293 in the Canadian Prairies.

294 The correlation coefficients between the mean regional precipitation anomaly over Canadian
295 Prairies and MJO-4 indices and MEI from May to August are shown in Table 1. The correlation
296 between MEI alone and the precipitation anomalies is not significant. The correlation between MJO-4
297 and precipitation in the Prairies is 0.18 with a p-value of 0.023, which indicates that stronger tropical
298 convection in the equatorial region ~~centred~~ around 140°E favours less precipitation in the Canadian
299 Prairies from May to August. When NINO4 is larger than 0, the correlation between MJO-4 and ~~the~~
300 growing season precipitation is 0.33 with a p-value of 0.0015. Conversely, the correlation between
301 MJO-4 and Canadian Prairie precipitation is -0.01 when NINO4 < 0.

302 The scatter plot in Fig. 5 shows the distribution of monthly precipitation anomaly versus MJO-4
303 index and NINO4 index. Circled asterisk denotes a month with precipitation anomaly larger than 18
304 mm/month and the red (blue) circles denote a negative (positive) precipitation anomaly. The criterion
305 for precipitation anomaly to be emphasized by the circles is roughly one-third of the mean monthly
306 precipitation in the growing season. The size of the circle represents the magnitude of the monthly
307 precipitation anomalies ~~with 6 mm/month interval~~. The bottom-right ~~quadrant~~, indicated by shading,
308 ~~shows that~~ negative MJO-4 corresponds to ~~many more dry months than wet months under NINO4 > 0~~
309 ~~conditions~~. We noticed that some significant dry months are not in the shaded area, which corresponds
310 to the dry months occurring during La Nina or in the period after the mature phase of El Nino (Bonsal *et*
311 *al.* 1999). Summer drought in the Prairies can occur in both phases of ENSO or any other teleconnection
312 indices. For example, for the summer drought that happened in the Prairies from 1999 to 2005, the
313 large-scale anomalous patterns of SST first showed La Nina conditions and then became a weak El Nino
314 in the latter half of the period (Hanesiak *et al.* 2011). Bonsal and Wheaton (2005) showed that the
315 tropospheric atmospheric circulation patterns in 2001 and 2002 lacked the typical meridional flow in the

Deleted: centered

Deleted:

Deleted:

Deleted:

Deleted: region

Deleted: under NINO4 > 0 condition,

Deleted: a quadrant that have

323 North Pacific and North America during the drought in western Canada. Their results show that the
324 drought in 1999-2005 was related to the expansion of the continuous drought happened in the US to the
325 north.

326 The impact of ENSO on the growing season precipitation over Canadian Prairies is investigated
327 through Fig. 6. The box-percentile plot in Fig. 6 shows the distribution of monthly Canadian Prairies'
328 precipitation anomalies from May to August along with different ENSO conditions. In general, under El
329 Nino and neutral ENSO conditions, the precipitation anomalies are centred around 0, and there is no
330 bias toward either end. Under La Nina condition, the mean precipitation has a positive bias. There are
331 only 10 summer months under La Nina condition, whereas there are 71 months under El Nino and
332 neutral conditions.

333 The distributions of precipitation anomalies versus MJO-4 index under different ENSO
334 conditions are shown in Fig. 7. For $\text{NINO4} > 0$, the precipitation anomaly has a negative tendency when
335 $\text{MJO-4} < -0.3$. With $\text{NINO4} < 0$, there is no negative tendency for $\text{MJO-4} < -0.3$. Therefore, Fig. 6 and 7
336 agrees with the significant correlation between precipitation and MJO-4 under $\text{NINO4} > 0$, relative to
337 ENSO in Table 1.

338 The correlation between MJO-4 and the Prairies' precipitation during the growing season leads
339 us to investigate the underlying circulation anomalies. Fig. 8 presents the regressed stream function and
340 wind field at 200 hPa in the mid-latitudes (north of 30°N) on the negative MJO-4 index from May to
341 August under warm NINO4 SST condition ($\text{NINO4} > 0.5$). In the tropics (10°S - 20°N), during Northern
342 Hemisphere summer, the OLR, velocity potential, and divergent wind vector are presented. Only
343 regression patterns having p-values lower than 0.05 are plotted for OLR and velocity potential. The
344 negative MJO-4 index corresponds to a negative anomaly in OLR, stronger convection and larger than
345 average divergence at 200 hPa in the region centre around 150°E . The strong convection anomaly

357 ~~centres~~ around 150°E, 5°N with divergent wind extending well into the subtropics in the Northern
 358 Hemisphere. The positive GPH/stream function anomaly extended from Japan to central Pacific is
 359 associated with the enhanced convection and divergence in the upper troposphere over the western
 360 tropical-subtropical Pacific. A Rossby wave train linked to the OLR anomaly and strong divergence in
 361 the western Pacific propagate eastward into North America, ~~in the extratropics~~. To better demonstrate the
 362 propagation of the wave train, we conducted a ray tracing ~~experiment~~ of stationary Rossby wave
 363 following the nondivergent barotropic Rossby wave theory of Hoskins and Karoly (1981) and Hoskins
 364 and Ambrizzi (1993). Equation 1 describes the group velocity, which ~~represents~~ the propagation of wave
 365 activity. C_{gx} and C_{gy} are the group velocity components on zonal and meridional directions; \bar{U} and \bar{V}
 366 are the mean zonal and meridional winds; q is the mean absolute vorticity; K , k , l are the total wave
 367 number, zonal wavenumber, and meridional wavenumber, respectively. The ray path is integrated using
 368 a fourth-order Runge-Kutta method.

$$C_{gx} = \bar{U} + \frac{(k^2 - l^2)q_y - 2klq_x}{K^4}$$

$$C_{gy} = \bar{V} + \frac{(k^2 - l^2)q_x + 2klq_y}{K^4}$$

Equation 1

369
 370
 371
 372 Under ~~the~~ average conditions in May-August derived from ERA-Interim at 200 hPa with
 373 NINO4 > 0.5 or NINO4 < -0.5, we released rays with a total wavenumber matching with the mean flow
 374 at the extratropical location of the OLR anomaly (140°E-150°E, 25°N-30°N). For quasi-stationary
 375 waves, the wavenumber is determined by the basic zonal flow and background absolute vorticity
 376 gradient through the Rossby wave dispersion relation. For NINO4 > 0.5 May-August condition, $K =$

~~Deleted: centers~~

~~Deleted: °~~

~~Deleted: °~~

~~Deleted:~~

~~Deleted: represent~~

~~Deleted:~~

$$C_{gx} = \bar{U} + \frac{(k^2 - l^2)q_y - 2klq_x}{K^4}$$

$$C_{gy} = \bar{V} + \frac{(k^2 - l^2)q_x + 2klq_y}{K^4}$$

Equation 1

~~Deleted: °~~

~~Deleted: °~~

~~Deleted: °~~

~~Deleted: °~~

391 4.14. With this total wavenumber and launching angle from 0- 60° relative to the zonal direction,
392 Rossby wave rays (coloured by red, orange to blue according to their angle from 0° to 60°) released at
393 140°W, 20°N can propagate successfully to the western Canada for those with smaller launching angles
394 (< 30°) as shown the bottom plot in Fig. 9. With NINO4<-0.5, the zonal wind in the source region is
395 weaker, and the meridional gradient of absolute vorticity is stronger due to its relative further southern
396 position to the subtropical jet. The total wavenumber for stationary Rossby waves is 6.2, determined by
397 the mean May-August condition for NINO4 < -0.5. The waves with shorter wavelength tend to be
398 evanescent near the source region as shown in the top plot in Fig. 9. However, there is no significant
399 difference in ray-path under NINO4 < -0.5 condition compared to NINO4 > 0.5, if the source
400 wavenumbers are set to the same value (results not shown). The changes in the mean conditions in the
401 midlatitudes away from the source region from El Nino to La Nina are not sufficient to alter the
402 propagation condition for quasi-stationary Rossby waves.
403

Deleted: °

Deleted: colored

Deleted: °

Deleted: °)

Deleted: °

Deleted: °

Deleted: ,

404 4 Discussion

405 Summer of 2015 is the first summer after the developing of El Nino during 2014-2015 winter.
406 Though the upper-level GPH pattern, seen in summer 2015, can be attributed to the SST modes in the
407 Pacific, namely ENSO and NPM, the precipitation in the Western Canadian Prairies is not strongly
408 correlated with either. Bonsal and Lawford (1999) found that more extended dry spells tend to occur in
409 the Canadian Prairies during the second summer following the mature stage of the El Nino events. The
410 winter precipitation in Canada has a strong connection to ENSO (Shabbar *et al.* 1997), whereas summer
411 precipitation, in most regions of western Canada (except the coast of British Columbia and Southern

Deleted: Prairie

420 Alberta), does not have a significant correlation with ENSO. This is consistent with our investigation
421 using instrumental records from 1948 to 2016.

422 Growing season precipitation in the Canadian Prairies is affected by many factors. Precipitation
423 deficits can occur under various circulation and lower boundary conditions. Thus, it is not expected that
424 a universal condition for all the significant droughts in the region can be identified. In fact, extreme
425 drought events have been found in both El Nino and La Nina years. A previous study by Bonsal and
426 Lawford (1999) indicates the meteorological drought often occurs after the mature phase of El Nino,
427 which is not the case for 2015. The associated anomaly in the North Pacific represented by NPM
428 positive phase is consistent with their results. The direct linkage between ENSO and the summer
429 precipitation in the Canadian Prairies is not clear. In fact, the correlation between MEI and the
430 precipitation in the investigated region is -0.096 (p=0.239, sample size = 152). The investigated region's
431 growing season precipitation does not possess a significant correlation with ENSO, which is consistent
432 with other researchers' findings (Dai and Wigley 2000).

433 The regression pattern is consistent with stationary Rossby wave theory as shown in a hierarchy
434 of theoretical and modelling studies (Karoly *et al.* 1989, Simmons *et al.* 1983, Hoskins and Ambrizzi
435 1993, Ambrizzi and Hoskins 1997, Held *et al.* 2002). A similar wave train extends from the western
436 Pacific toward extra-tropical South America but at lower latitudes compared to its counterpart in the
437 Northern Hemisphere (not shown). The node of the wave train in Western Canada and Northwest
438 Pacific of the US corresponds to an anomalous ridge, which is in-phase of El Nino forcing. When the
439 convection in the region associated with MJO-4 is weaker than normal ($MJO-4 > 0$), a wave train with
440 the opposite sign will reach western Canada which then counteracts the El Nino forcing. Thus, the weak
441 correlation between Canadian Prairie precipitation and ENSO is understandable as MJO plays an
442 additional role that enhances or cancels out the GPH anomaly caused by El Nino.

448 In the mid-latitude North America, the atmospheric response to the tropical forcing in the
449 western Pacific depends on the mean circulation condition associated with tropical SST. Intraseasonal
450 tropical convection oscillation in the western Pacific associated with the MJO-4 index cannot determine
451 the sign of the precipitation anomaly in the Prairies alone. Both warm SST in central Pacific and strong
452 tropical convection in western Pacific and Maritime Continent are essential to cause a significant
453 precipitation deficit in the western Canadian Prairies. Warm SST in central Pacific causes an eastward
454 expansion of Pacific warm pool that favours enhanced MJO activity in the western-central Pacific
455 (Hendon *et al.* 1999, Marshall *et al.* 2016). As shown by the ray-tracing result, the NINO4 also affects
456 the wavenumber of the quasi-stationary Rossby waves over the source region in the western Pacific.
457 Under warm NINO4, the wavenumbers tend to be smaller due to stronger westerly in the source region
458 and these waves can propagate northeastward into western Canada. Conversely, from May to August
459 under cold NINO4, the westerly is weaker, and the meridional vorticity gradient is stronger in the
460 subtropics near the source region. These mean flow conditions correspond to waves with larger
461 wavenumbers that cannot propagate across the dateline.

462 In the year 2015, the SST anomaly in the Pacific (e.g. ENSO, NPM) coincided with the
463 anomalous ridge on the west coast of Canada. This positive GPH anomaly was associated with the
464 strong negative MJO4 indices, it then caused a blocking pattern and suppressed precipitation in the
465 Canadian Prairies in the early summer, through the mechanism discussed above. Although the El Nino
466 continued to strengthen in July and August 2015, the active convection associated with MJO in the
467 western Pacific propagated eastward into the central Pacific. As the convection in the western
468 Pacific/Maritime Continent waned, the precipitation in the Canadian Prairie returned to slightly above
469 normal in July.

470

Deleted: forced

Deleted: .

473 **5 Conclusions**

474 The cause of the 2015 summer precipitation deficit in the western Canadian Prairies is
475 investigated in relation to atmospheric circulation anomalies, SST, and intraseasonal tropical convection
476 oscillation, MJO. The drought in western Canada is immediately related to an anomalous upper-level
477 ridge that persisted over the west coast of Canada and Alaska since fall 2014. This ridge was likely
478 associated with a developing El Nino that was enhanced by the MJO.

Deleted:

479 In general, MJO-4 indices demonstrated significant correlation with the meteorological drought
480 over the Canadian Prairies from May to August when the SST in the central Pacific is warm (NINO4 >
481 0), which also corresponds to a stronger MJO amplitude in boreal summer. Our study discovered that
482 MJO phase/strength is connected to the anomalous ridge over western Canada through the propagation
483 of stationary Rossby waves from the western Pacific when NINO4 is positive. Though seasonally MJO
484 is weaker in summer, the spring and early summer MJO amplitudes are larger than normal when the
485 central Pacific SST is warmer than normal (NINO4 >0). The teleconnection between the Canadian
486 Prairie precipitation deficit and MJO is stronger when NINO4 is positive. The underlying cause of this
487 significant correlation between MJO-4 indices and the prairie precipitation in May-August is a
488 stationary Rossby wave train originating from the Maritime Continent and western Pacific which
489 propagates into Canada. The raytracing experiments show the main difference between a warm phase of
490 NINO4 and a cold phase is the changes in stationary Rossby wave wavenumber over the source region.

Deleted: happened
Deleted: west
Deleted: warm
Deleted: presented
Deleted:) with strong
Deleted: wave
Deleted: amplitude is

491 Under NINO4 > 0.5 May-August conditions, the total wavenumber is about 4 and can propagate into
492 western Canada if they are oriented relatively zonally. Compared to NINO4 > 0.5, NINO4 < -0.5
493 corresponds to a weaker zonal wind and stronger meridional gradient of absolute vorticity in the
494 subtropics of the source region (140°-150°E). Hence, the wavenumbers of stationary Rossby waves
495 from the source region under NINO4 < -0.5 are larger (about 6), and these waves fail to reach the

Deleted: condition
Deleted: -150E), hence

507 Western Hemisphere. The intra-seasonal predictability of the growing season precipitation in the
508 Canadian Prairies can be potentially improved by including the MJO amplitude and phase factors for
509 medium-range/intra-seasonal projection in addition to ENSO effect especially when the central-Pacific
510 SST is warm.

511

512 **Acknowledgment**

Deleted: Acknowledgement

513 We gratefully acknowledge the Natural Sciences and Engineering Research Council of Canada
514 (NSERC) for funding the Changing Cold Regions Network (CCRN) through their Climate Change and
515 Atmospheric Research (CCAR) Initiative. Dr. Zhenhua Li is supported by the Probing the Atmosphere
516 of the High **Arctic** project sponsored by the NSERC. Dr. Yanping Li gratefully acknowledges the
517 support from the Global Institute of Water Security at the University of Saskatchewan. This research is
518 also supported by Environment and Climate Change Canada (ECCC).

Deleted:

Deleted: Arctic

Deleted:

Deleted:

519

520

521

527 **References**

528 Ambrizzi T and Hoskins B J 1997: Stationary Rossby-Wave Propagation in a Baroclinic Atmosphere,
529 *Quart. J. Roy. Meteor. Soc.*, **123** 919–28.

530
531 Andrews, E.D., R.C. Antweiler, P.J. Neiman, and F.M. Ralph, 2004: Influence of ENSO on Flood
532 Frequency along the California Coast. *J. Climate*, **17**, 337–348, doi: 10.1175/1520-0442(2004)017.

Deleted:

533
534 Bonsal, B.R., Chakravarti, A.K. and Lawford, R.G. 1993: Teleconnections between North Pacific SST
535 Anomalies and Growing Season Extended Dry Spells on the Canadian Prairies, *Int. J. Climatol.*, **13**,
536 865-878.

537
538 Bonsal, B.R., Zhang, X. and Hogg, W.D., 1999: Canadian Prairie growing season precipitation
539 variability and associated atmospheric circulation, *Climate Research*, **11**(3), 191-208.

540
541 Bonsal B and Lawford R 1999: Teleconnections between El Niño and La Niña Events and Summer
542 Extended Dry Spells on the Canadian Prairies, *International Journal of Climatology*, **19**, 1445–58.

543
544 Bonsal B R, Shabbar A and Higuchi K, 2001: Impacts of Low Frequency Variability Modes on
545 Canadian Winter Temperature, *Int. J. Climatol.* **21**, 95–108.

546 Bonsal, B.R. and E. Wheaton, 2005: Atmospheric circulation comparisons between the 2001 and 2002
547 and the 1961 and 1988 Canadian Prairie droughts. *Atmosphere-Ocean*, **43** (2): 163–172.

Deleted: BONSAL

Deleted: WHEATON.

548 Bonsal B R and Regier M, 2007: Historical Comparison of the 2001/2002 Drought in the Canadian
549 Prairies, *Climate Research*, **33**, 229-242.

553 Bonsal, B R, Aider, R, Gachon, P and Lapp S, 2013: An Assessment of Canadian Prairie Drought: Past,
554 Present, and Future, *Climate Dynamics*, **41**, 501–516.

555

556 Carbone R. E., Yanping Li, 2015: Tropical Oceanic Rainfall and Sea Surface Temperature Structure:
557 Parsing Causation from Correlation in the MJO, *Journal of Atmospheric Science*, Vol. 72, No. 7, 2703–
558 2718.

559

560 Cassou C, 2008: Intraseasonal Interaction Between the Madden-Julian Oscillation and the North
561 Atlantic Oscillation, *Nature*, **455** 523–7.

562

563 Dai A and Wigley T M L, 2000: Global Patterns of ENSO-Induced Precipitation, *Geophys. Res. Lett.*,
564 **27** 1283–6.

565

566 Dee D P, Uppala S M, Simmons A J, Berrisford P, Poli P, Kobayashi S, Andrae U, Balmaseda M A,
567 Balsamo G, Bauer P, Bechtold P, Beljaars A C M, Berg L van de, Bidlot J, Bormann N, Delsol C,
568 Dragani R, Fuentes M, Geer A J, Haimberger L, Healy S B, Hersbach H, Hólm E V, Isaksen L, Kållberg
569 P, Köhler M, Matricardi M, McNally A P, Monge-Sanz B M, Morcrette J-J, Park B-K, Peubey C,
570 Rosnay P de, Tavolato C, Thépaut J-N, and Vitart F, 2011: The ERA-Interim Reanalysis: Configuration
571 and Performance of the Data Assimilation System, *Quarterly Journal of the Royal Meteorological
572 Society*, **137**, 553–97.

573

574 Dey B, 1982: Nature and Possible Causes of Droughts on the Canadian Prairies-Case Studies, *Journal of
575 Climatology*, **2**, 233–49.

576

577 Garfinkel C I, Feldstein S B, Waugh D W, Yoo C and Lee S, 2012: Observed Connection Between
578 Stratospheric Sudden Warmings and the Madden-Julian Oscillation, *Geophys. Res. Lett.*, **39**.

579
580 Hanesiak, J. M., Stewart, R. E., Bonsal, B. R., Harder, P., Lawford, R., Aider, R., *et al.* (2011).
581 Characterization and Summary of the 1999–2005 Canadian Prairie Drought. *Atmosphere-Ocean*, **49**(4),
582 421–452. <http://doi.org/10.1080/07055900.2011.626757>

Deleted: <http://doi.org/10.1080/07055900.2011.626757>

583
584 Hartmann D L, 2015: Pacific Sea Surface Temperature and the Winter of 2014, *Geophys. Res. Lett.*, **42**,
585 1894–902.

586
587 Held I. M., Ting M. and Wang H., 2002: Northern Winter Stationary Waves: Theory and Modeling *J.*
588 *Climate*, **15**, 2125–44.

589
590 Hendon, H. H., C. Zhang, and J. D. Glick, 1999: Interannual variation of the Madden-Julian Oscillation
591 during Austral summer, *J. Clim.*, **12**, 2538–2550

592
593 Hong, C. C., Hsu, H. H., Tseng, W.-L., Lee, M. Y., Chow, C.-H., & Jiang, L.-C. 2017: Extratropical
594 Forcing Triggered the 2015 Madden–Julian Oscillation–El Niño Event. *Sci. Rep.* **7**, 46692; doi:
595 10.1038/srep46692.

596 Hoskins B J and Ambrizzi T, 1993: Rossby Wave Propagation on a Realistic Longitudinally Varying
597 Flow. *J. Atmos. Sci.* **50** 1661–71

598 Hoskins, B.J. and D.J. Karoly, 1981: [The Steady Linear Response of a Spherical Atmosphere to](#)
599 [Thermal and Orographic Forcing](#). *J. Atmos. Sci.*, **38**, 1179–1196

Deleted: The Steady Linear Response of a Spherical Atmosphere to Thermal and Orographic Forcing

Deleted: [https://doi.org/10.1175/1520-0469\(1981\)038<1179:TSLROA>2.0.CO;2](https://doi.org/10.1175/1520-0469(1981)038<1179:TSLROA>2.0.CO;2)

605 Hoskins, B.J. and T. Ambrizzi, 1993: [Rossby Wave Propagation on a Realistic Longitudinally Varying Flow](#), *J. Atmos. Sci.*, 50, 1661–1671,

Deleted: [Rossby Wave Propagation on a Realistic Longitudinally Varying Flow](#).

Deleted: [https://doi.org/10.1175/1520-0469\(1993\)050<1661:RWPOAR>2.0.CO;2](https://doi.org/10.1175/1520-0469(1993)050<1661:RWPOAR>2.0.CO;2)

607
608 Huang B, Banzon V F, Freeman E, Lawrimore J, Liu W, Peterson T C, Smith T M, Thorne P W,
609 Woodruff S D and Zhang H-M, 2015: Extended Reconstructed Sea Surface Temperature Version 4
610 (ERSST. v4). Part I: Upgrades and Intercomparisons *Journal of Climate*, **28**, 911–30.

611 Kalnay E, Kanamitsu M, Kistler R, Collins W, Deaven D, Gandin L, Iredell M, Saha S, White G,
612 Woollen J, Zhu Y, Chelliah M, Ebisuzaki W, Higgins W, Janowiak J, Mo K, Ropelewski C, Wang J,
613 Leetmaa A, Reynolds R, Jenne R and Joseph D, 1996: The NCEP/NCAR 40-Year Reanalysis Project
614 *Bull. Amer. Meteor. Soc.* **77** 437–71

615
616 Karoly D J, Plumb R A, and Ting M, 1989: Examples of the Horizontal Propagation of Quasi-Stationary
617 Waves. *J. Atmos. Sci.* **46** 2802–11

618
619 Lee M Y, Hong C C and Hsu H H 2015: Compounding Effects of Warm Sea Surface Temperature and
620 Reduced Sea Ice on the Extreme Circulation Over the Extratropical North Pacific and North America
621 During the 20132014 Boreal winter *Geophys. Res. Lett.*, **42**, 1612–8.

622
623 Li Y., Richard E. Carbone, 2012: Excitation of rainfall over the tropical western Pacific. *Journal of*
624 *Atmospheric Science*, Vol. 69, No. 10, 2983–2994.

625
626 Li Y., Kit Szeto, Ron Stewart, Julie Theriault, Liang Chen, Bob Kochtubajda, Anthony Liu, Sudesh
627 Boodoo, Ron Goodson, Curtis Mooney, Sopan Kurkute, 2017: The June 2013 Alberta Catastrophic

632 Flooding: Water vapor transport analysis by WRF simulation. *Journal of Hydrometeorology*, Vol. 18,
633 2057-2078.

634

635 Li Z., Alan Manson, Yanping Li, Chris Meek, 2017: Circulation Characteristics of Persistent Cold
636 Spells in Central-Eastern North America. *Journal of Met. Res.*, Vol. 31, 250-260.

637

638 Liu J, Stewart R E and Szeto K K, 2004: Moisture Transport and Other Hydrometeorological Features
639 Associated With the Severe 2000/01 Drought Over the Western and Central Canadian Prairies *Journal*
640 *Of Climate*, **17**, 305–19.

641

642 Liu A., C. Mooney, K. Szeto, J. M. Thériault, B. Kochtubajda, R.E. Stewart, S. Boodoo, R. Goodson, Y.
643 Li, J. Pomeroy, 2016: The June 2013 Alberta Catastrophic Flooding Event: Part 1 – Large scale features.
644 *Hydrological Process*, 2016, 30, 4899–4916

645

646 Lorenz, D.J. and D.L. Hartmann, 2006: The Effect of the MJO on the North American Monsoon. *J.*
647 *Climate*, **19**, 333–343, doi: 10.1175/JCLI3684.1.

648 Madden R A and Julian P R, 1971: Detection of a 40-50 Day Oscillation in the Zonal Wind in the
649 Tropical Pacific, *J. Atmos. Sci.*, **28**, 702–8

650 Marshall, A. G., H. H. Hendon, and G. Wang, 2016: On the role of anomalous ocean surface
651 temperatures for promoting the record Madden-Julian Oscillation in March 2015, *Geophys. Res. Lett.*,
652 43,472–481.

653

654 Riddle E E, Stoner M B, Johnson N C, L'Heureux M L, Collins D C and Feldstein S B, 2013: The
655 Impact of the MJO on Clusters of Wintertime Circulation Anomalies Over the North American region
656 *Climate Dynamics*, **40**, 1749–66.

657

658 Rodney, M., Lin, H., & Derome, J. 2013: Subseasonal Prediction of Wintertime North American
659 Surface Air Temperature during Strong MJO Events. *Monthly Weather Review*, **141**(8), 2897–2909.

660 <http://doi.org/10.1175/MWR-D-12-00221.1>.

Deleted: <http://doi.org/10.1175/MWR-D-12-00221.1>.

661

662 Ropelewski C F and Halpert M S 1986: North American Precipitation and Temperature Patterns
663 Associated with the El Niño/Southern Oscillation (ENSO), *Monthly Weather Review*, **114**, 2352–62.

664

665 Shabbar, A., Bonsal, B. and Khandekar, M., 1997: Canadian precipitation patterns associated with the
666 Southern Oscillation. *Journal of Climate* 10:3016-3027.

667

668 Shabbar A and Skinner W, 2004: Summer Drought Patterns in Canada and the Relationship to Global
669 Sea Surface Temperatures, *Journal of Climate*, **17**, 2866–80.

670

671 Shabbar A, Bonsal B R and Szeto K, 2011: Atmospheric and Oceanic Variability Associated with
672 Growing Season Droughts and Pluvials on the Canadian Prairies, *Atmosphere-Ocean*, **49**, 339–55.

673

674 Simmons A J, Wallace J M and Branstator G W, 1983: Barotropic Wave Propagation and Instability,
675 and Atmospheric Teleconnection Patterns, *J. Atmos. Sci.*, **40**, 1363–92.

676

677

679 Szeto, K., X. Zhang, R.E. White, and J. Brimelow, 2016: The 2015 Extreme Drought in Western
680 Canada. *Bull. Amer. Meteor. Soc.*, **97**, S42–S46, <https://doi.org/10.1175/BAMS-D-16-0147.1>.

681
682 Wang S Y, Hipps L, Gillies R R and Yoon J-H, 2014: Probable Causes of the Abnormal Ridge
683 Accompanying the 2013-2014, California Drought: ENSO Precursor and Anthropogenic Warming
684 footprint *Geophys. Res. Lett.*, **41** 3220–6.

685
686 Xie P and Arkin P A, 1997: Global Precipitation: A 17-year Monthly Analysis Based on Gauge
687 Observations, Satellite Estimates, and Numerical Model Outputs. *Bulletin of the American
688 Meteorological Society*, **78**, 2539–58.

689
690 Xue Y, Higgins W and Kousky V 2002: Influences of the Madden-Julian Oscillations on Temperature
691 and Precipitation in North America during ENSO-neutral and Weak ENSO Winters, *Proc. workshop on
692 prospects for improved forecasts of weather and short-term climate variability on subseasonal (2 week
693 to 2 month) time scales*.

694
695 Wheaton, E, Wittrock V, Kulshreshtha S, Koshida G, Grant C, Chipanshi A, Bonsal BR, 2005: Lessons
696 Learned from the Drought Years of 2001 and 2002: Synthesis Report. Agriculture and Agri-Food
697 Canada, Saskatchewan Research Council Publ No. 11602–46E03, Saskatoon.

698
699 Wheeler, M. C., & Hendon, H. H., 2004: An all-season real-time multivariate MJO index: Development
700 of an index for monitoring and prediction. *Monthly Weather Review*, **132**(8), 1917–1932.

703 Wolter, K., 1987: The Southern Oscillation in surface circulation and climate over the tropical
704 Atlantic, Eastern Pacific, and Indian Oceans as captured by cluster analysis. *J. Climate Appl.*
705 *Meteor.*, 26, 540-558.

706

707 Wolter, K. and M.S. Timlin, 1993: Monitoring ENSO in COADS with a seasonally adjusted principal
708 component index. *Proc. of the 17th Climate Diagnostics Workshop*, Norman, OK,
709 NOAA/NMC/CAC, NSSL, Oklahoma Clim. Survey, CIMMS and the School of Meteor., Univ. of
710 Oklahoma, 52-57.

711

712 Zhang C, 2005: Madden-Julian Oscillation *Reviews of Geophysics*, **43**.

713

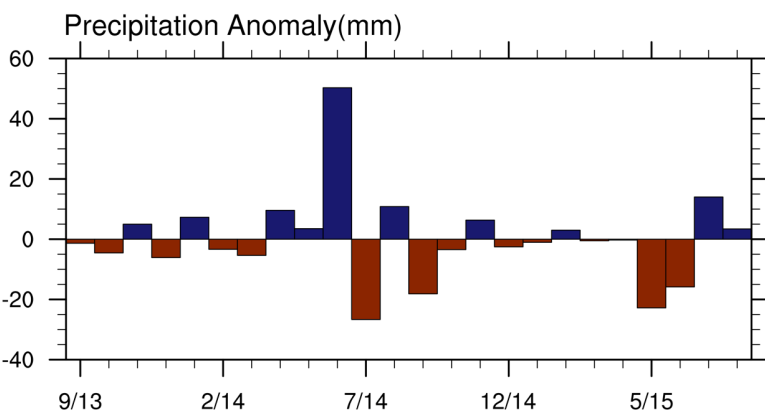
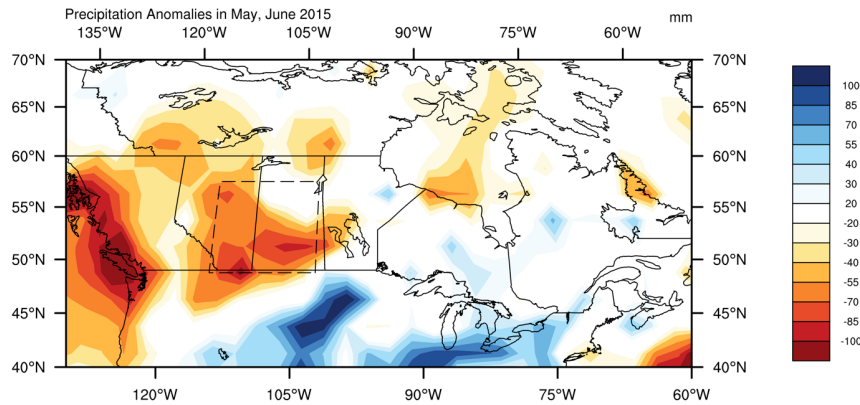
714

715

716 Table 1 Correlation between mean precipitation anomaly in the Prairies from CMAP and MEI, MJO
717 indices 4. MJO indices and CMAP are from 1979 to 2016.

	Correlation	p-value	No. of sample
MEI	-0.096	0.24	156
MJO-4	0.18	0.023	156
MJO-4(NINO4>0)	0.33	0.0015	90
MJO-4(NINO4<0)	-0.01	0.94	66

718



719

720 Fig. 1 Top: Precipitation anomalies (mm) from CMAP over the region (115 W-102.5 W, 50 N-57.5 N)
 721 during May and June 2015. Bottom: time series of monthly precipitation anomaly over boxed region
 722 between September 2013 and August 2015.

723

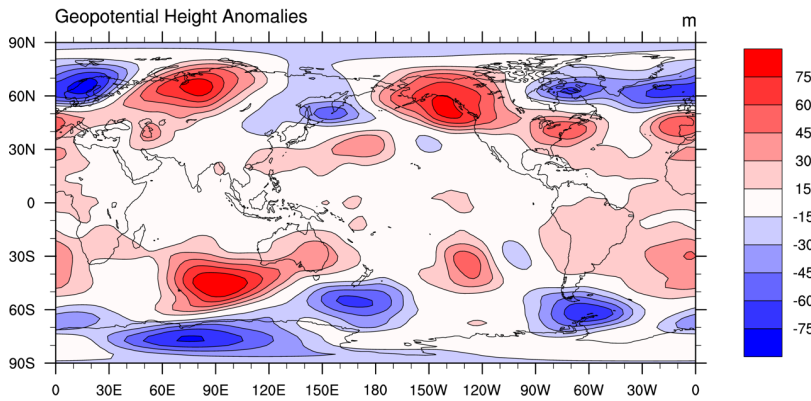
724

725

726

727

Mean GPH Anomaly of May, June 2015



729 Fig. 2 NCEP GPH anomaly at 500hPa during May and June 2015 when the precipitation deficit was the
730 largest.

731

732

733

734

735

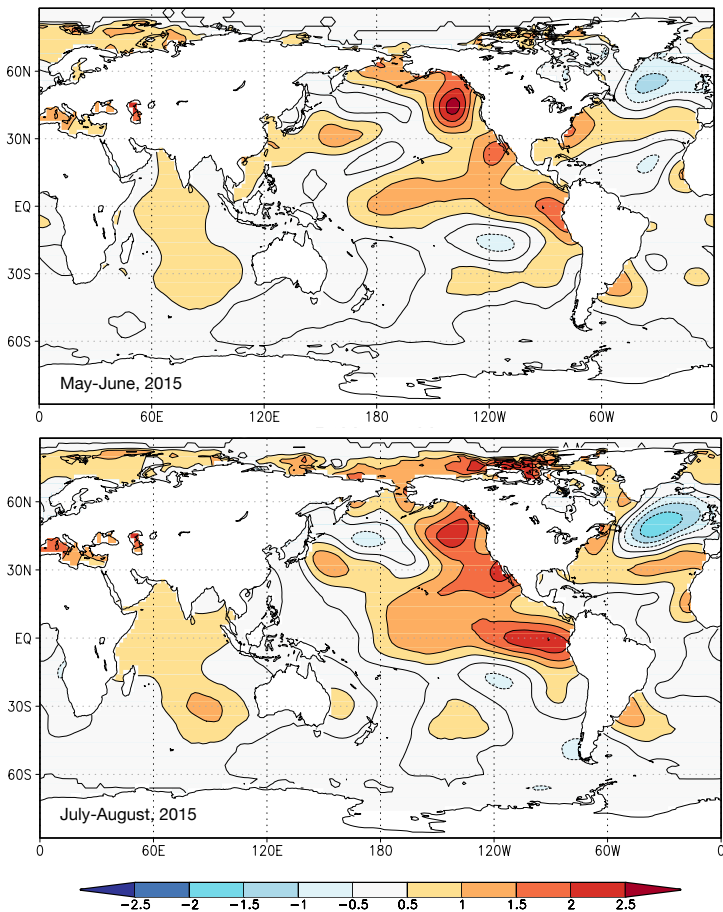
736

737

738

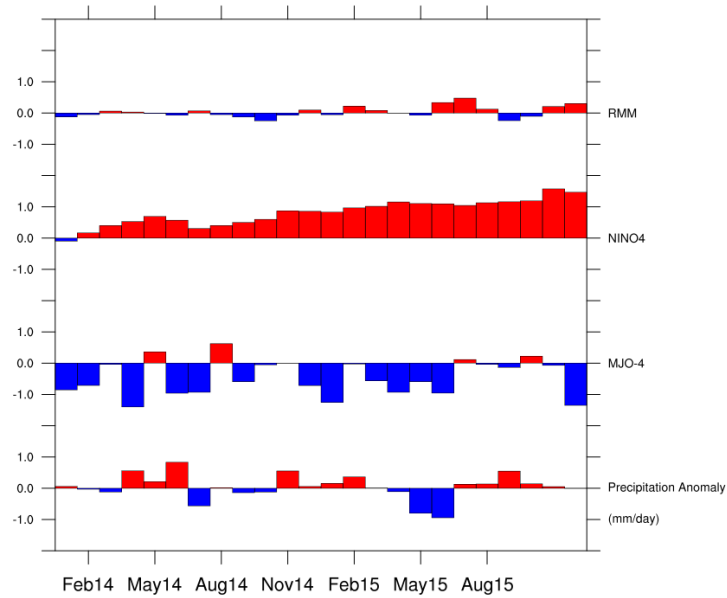
739

740



741

742 Fig. 3 The mean SST anomaly ($^{\circ}\text{C}$) from ERSST v4 for May-June and July-August 2015.



743

744 Fig. 4 RMM amplitude anomaly, NINO4, MJO 4 indices and precipitation anomaly of [the](#) Canadian
745 Prairies from January 2014 to Dec 2015.

746

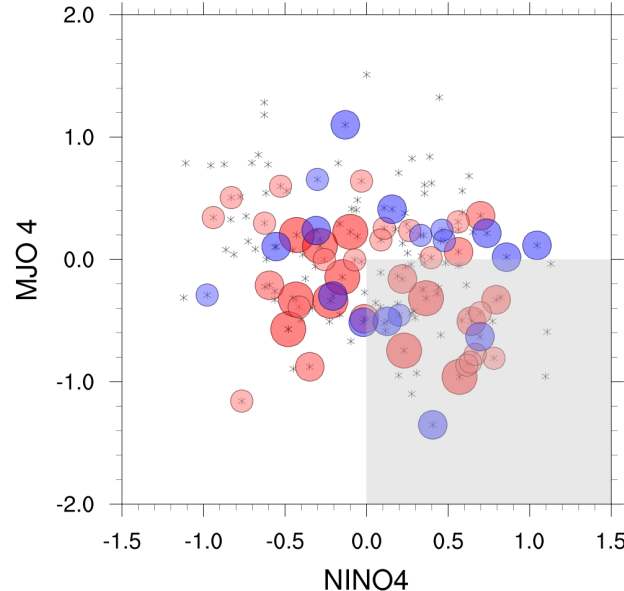
747

748

749

750

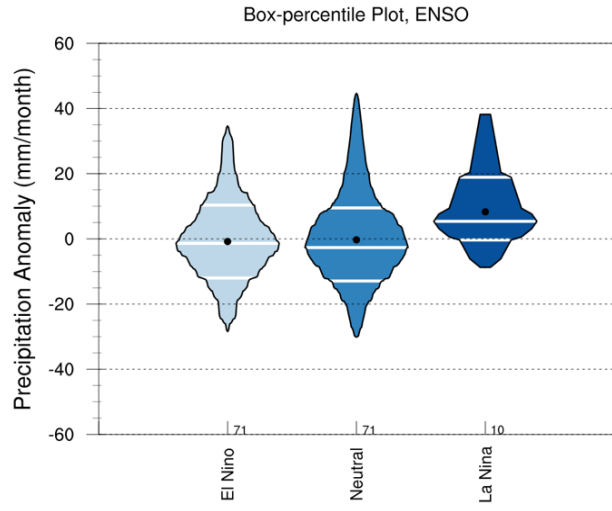
751



752

753 Fig. 5 The scatter plot of monthly precipitation anomaly (mm/month) as a function of MJO-4 and
754 NINO4. Each asterisk represents a month from May to August 1979-2016. Circled asterisk denotes a
755 month with precipitation anomaly larger than 18 mm/month. The blue circles are months with positive
756 precipitation anomaly and the red circles are months with negative precipitation anomaly. The sizes of
757 circles denote the magnitudes of the anomalies (large > 30 mm/month, medium > 24 mm/month,
758 small >18 mm/month). The shaded area denotes NINO4 > 0 and MJO-4 index < 0.

759



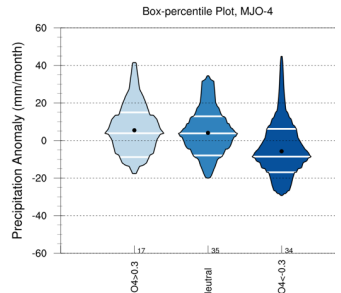
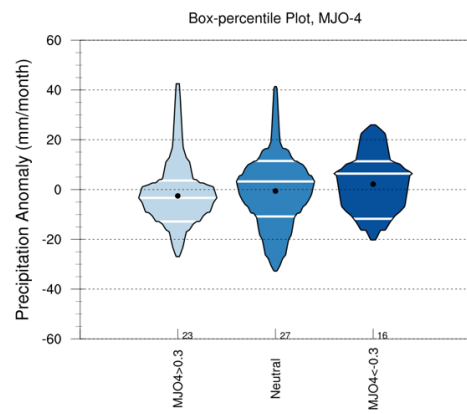
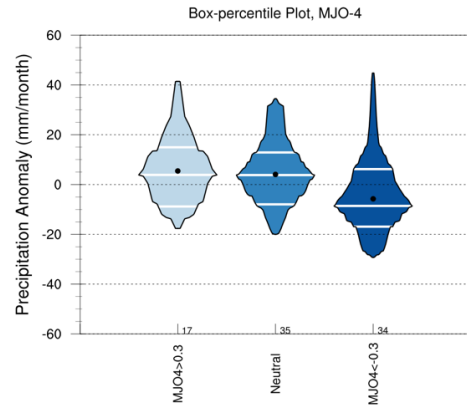
760

761 Fig. 6 The box-percentile plot of [the](#) Canadian Prairies precipitation anomaly during growing season
762 under different ENSO conditions.

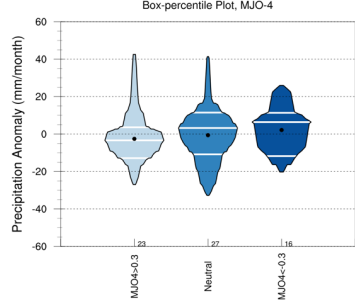
763

764

765



Deleted:



766

767

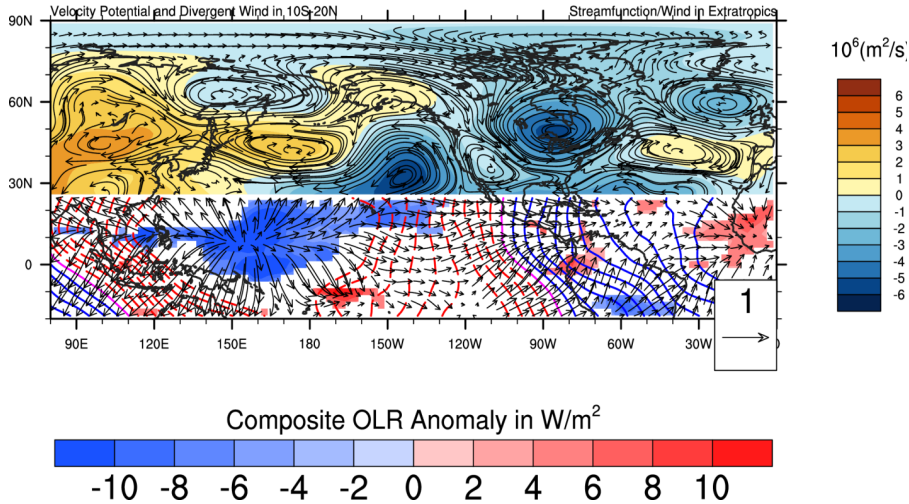
Fig. 7 Box-percentile plots of the Canadian Prairies' precipitation anomaly during growing season versus MJO-4 under warm NINO4 ($\text{NINO4} > 0$, top) and cold NINO4 ($\text{NINO4} < 0$, bottom) SST condition.

Deleted: left

Deleted: right

771

776



777

778

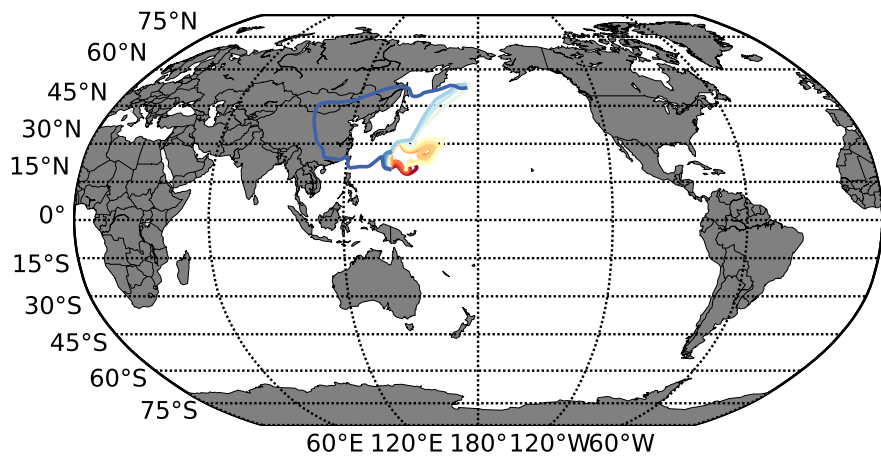
779 Fig. 8 The regression of stream function, wind field in the extratropics on negative MJO-4 for May-
780 August with $\text{NINO4} > 0.5$ condition. In the tropics, the regression of OLR, velocity potential, and
781 divergent wind on negative MJO-4 indices for May-August with $\text{NINO4} > 0.5$ condition. The shaded
782 region for the tropical OLR has p -value < 0.05 . Blue shading indicates active convection region. Red
783 dashed contour and solid blue contour corresponds to negative and positive velocity potential,
784 respectively.

785

786

787

788



789

Fig. 9: Ray-tracing result with total wavenumber specified by the mean flow 140-150W and 20-30N for

mean May-August condition with $\text{NINO4} < -0.5$ (top) and $\text{NINO4} > 0.5$ (bottom). Rays originate from 140E, 20N with angles ranging from 0 (red) to 60 degrees (dark blue) from zonal direction.

793